Eur. Phys. J. B **47**, 161–164 (2005)
DOI: 10.1140/epjb/e2005-00302-5

THE EUROPEAN PHYSICAL JOURNAL B

Purcell's "rotator": mechanical rotation at low Reynolds number

R. Dreyfus[1,a], J. Baudry[1,b], and H.A. Stone[2,c]

[1] Laboratoire Colloïdes et Matériaux Divisés, ESPCI et CNRS, UMR7612, UPMC, 10 rue Vauquelin, 75231 Paris Cedex 05, France
[2] Permanent Address: Division of Engineering and Applied Sciences, Harvard University, Cambridge, MA 02138, USA

Received 4 February 2005 / Received in final form 17 June 2005
Published online 21 September 2005 –

Abstract. An object consisting of three spheres, linked like the spokes on a wheel, can undergo a net rotational movement when the relative positions of the spheres proceed through a four-step cycle. This rotational motion is the analogue of the two-hinged swimmer originally proposed by Purcell (1977), which has served as a prototype for mechanical implementations of swimming. We also note that the rotational motion analysed here may be useful in the design of micromachines and has similarities to molecular-scale rotational motors that have been identified recently.

PACS. 87.19.St Movement and locomotion – 47.15.Gf Low-Reynolds-number (creeping) flows – 67.40.Hf Hydrodynamics in specific geometries, flow in narrow channels

The study of swimming microorganisms has generated a long and venerable literature, in part owing to the variety of strategies employed in nature. Early work by Taylor [1], which was later beautifully illustrated in the film "Low Reynolds number flows" [2], introduced many important physical ideas for quantifying self-propulsion in the viscously dominated flow limit. In particular, studies of low-Reynolds-number self-propulsion [3–6] have examined slender bodies, spherical squirmers, models for flagellated and ciliated microorganisms, etc. The impact of elasticity of the slender filaments on swimming motions has been described more recently [7–9] as have studies focused on optimal swimming strategies [10]. These ideas also have relevance to the design of micromachines for which it is important to consider both translational and rotational motions.

The basic fluid dynamical aspects of swimming in viscous fluids were popularized in the physics literature by Purcell [11]. In the low-Reynolds-number flow limit, the Navier-Stokes equations simplify to linear and stationary equations for the fluid velocity and pressure fields. One important consequence of this linearity and no-time dependence is that movements of a body that are strictly reversible in a kinematical sense can produce no net motion of the body after a complete cycle of the boundary motion. Thus, as Purcell discussed, a single-hinged "scallop", which simply opens and closes the hinge, cannot translate in the low-Reynolds-number flow limit. On the other hand, to illustrate how cyclic motions that are kinematically irreversible can produce net propulsion of force- and torque-free objects, Purcell introduced the idea of a two-hinged swimmer, which was analysed recently by Becker et al. [12]. A closely related idea is provided by a continuously turning corkscrew, which translates as a consequence of its rotation.

The important idea to take away from Purcell's two-hinged swimmer is that two degrees of freedom are sufficient to escape the reversibility constraint of self-propulsion for simple mechanical objects. An elegant extension of this idea was recently given by Najafi and Golestanian [13] who illustrated how strictly collinear movements of linked spheres may give rise to translation. An additional variant has been proposed by Avron et al. [14] who describe net translation of two linked spheres with time-periodic volume changes allowed. Here, we provide a similar example that illustrates rotation of a simple mechanical object with two degrees of freedom. Certain aspects of this rigid-body rotation by cyclic rearrangement of the individual components have similarity with recent descriptions and observations of molecular motors, which are discussed briefly at the end.

The mechanical example we provide here is illustrated in Figure 1 and is similar in spirit to that proposed recently for translation by Najafi and Golestanian [13]. The device consists of three spheres of radius R placed on an imaginary circle. Each sphere is connected to a rigid rod of length L and the rods are connected together at the centre P of the circle. Two internal engines act at the center

[a] e-mail: remi.dreyfus@espci.fr
[b] e-mail: jean.baudry@espci.fr
[c] e-mail: has@deas.harvard.edu

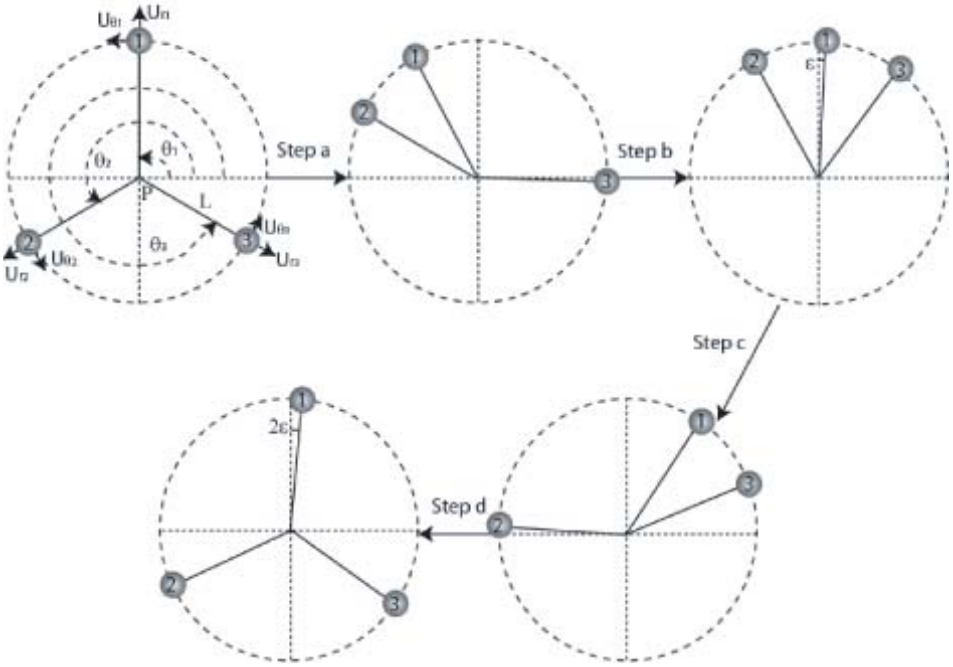

Fig. 1. Complete 4-step cycle of the proposed non-reciprocal motion of a rotational motor. The device experiences a net rotation after completion of a cycle.

as active elements and move the spheres closer or further apart in a non-reciprocal fashion, which, as we shall show, allows the whole system to rotate. If no external force is applied, this simple system also undergoes translational motion.

To begin with, the angle between each sphere is equal to 120°. The subsequent cyclic motion is divided into four distinct steps: in the first step (a) of the motion, the angle between spheres 1 and 2 decreases at a constant relative angular velocity ω. During this step, the relative position between spheres 1 and 3 does not change. In the second step (b), the angle between spheres 1 and 3 decreases at the relative angular velocity ω while the angle between 1 and 2 remains constant. In the third step (c), the angle between spheres 1 and 2 increases at the relative angular velocity ω to reach its initial value of 120°, while the angle between spheres 1 and 3 is fixed. Finally, in the last step (d), the angle between spheres 1 and 3 also increases at relative angular velocity ω to reach its initial value 120° while the angle between spheres 2 and 3 is kept fixed. After these four steps, the three spheres have the same relative angular positions as in step a and so describe a cycle in shape space. We refer to the "angular change" as the difference between the value of $\theta_j - \theta_1$ ($j = 2$ for steps a and c and $j = 3$ for steps b and d) taken at the end of the considered step and at the beginning of the same step. The "angular change" denoted by θ is the same for all four of the steps of the above cycle. We will demonstrate that after these four steps, in which the system has returned to its initial configuration, it has experienced a net rotation in the laboratory frame of reference. It is then natural to think about this model as the rotational equivalent of Purcell's two-hinged swimmer [11]. Further rotation of the object only requires that the cycle be repeated. Increasing the rate of rotation can be achieved by increasing ω and so decreasing the cycle time.

To understand why such a cyclic motion can induce a net rotation of the device, we first consider the case where the centre of the device is kept fixed, meaning that the whole system cannot undergo translational motion. In the viscous regime, a moving sphere interacts with the solvent and also with the other spheres through the solvent; the viscous force and torque acting on a sphere depends both on its own velocity and on the velocities and the positions of the other spheres. During the first step (a) of the motion, when sphere 2 is moving closer to sphere 1, spheres 1 and 3 are moving in the opposite angular direction in order to ensure the torque-free condition. For the same reason, during step b, spheres 1 and 2 move in the angular direction opposite to that of sphere 3. As spheres 1 and 2 are closer to each other during step b than spheres 1 and 3 during step a, the viscous forces on spheres 1 and 2 during step b is smaller than the viscous forces acting on spheres 1 and 3 during step a. Therefore sphere 1 is almost but not exactly back to its initial position at the end of step b and we denote by ε the small angle between the position of sphere 1 at the end of the second step and its initial position (Fig. 1). By considering the symmetry of the motion, sphere 1 rotates by the same angle during the third step as during the second step, and also step d, after a reflection, is identical to step a. Therefore, at the end of the entire four-step cycle, the device has experienced a net rotation 2ε. In order to investigate the dynamics quantitatively, we performed numerical calculations, whose elements are described next for the general case when both rotation and translation of the device are allowed.

We consider the translational motion of the spheres but neglect the influence of the connecting rods. At low Reynolds number, the governing equations are the Stokes equation and the incompressibility condition. Since both equations are linear, and if we denote by $\vec{r}_i$ the position vector of sphere i measured from the center P, then there is a linear tensor relation between the forces acting on each sphere $\vec{F}_i$ and their velocity $\vec{V}_i$ of the form,

$$\vec{F}_i = \sum_{j=1}^{3} H_{ij}\vec{V}_j, \text{ with } \begin{cases} H_{ii} = -6\pi\eta R I \\ H_{ij} = -6\pi\eta R \frac{3R}{4R_{ij}}(I + \hat{R}_{ij}\hat{R}_{ij}) \\ \hat{R}_{ij} = \frac{\vec{r}_i - \vec{r}_j}{\|\vec{r}_i - \vec{r}_j\|} \\ R_{ij} = \|\vec{r}_i - \vec{r}_j\| \end{cases} \quad (1)$$

where I is the identity tensor and η is the viscosity of the fluid. These equations account for the leading-order hydrodynamic influences and for interactions among each of the spheres treated as point forces ($R/L \ll 1$).

The coefficients H_{ij} relating forces and velocities are components of the Oseen's tensor, which is well known for spheres. If we denote $\vec{D}_i$ as the position of the center of sphere i measured from a fixed point in the laboratory frame, an additional linear tensor relation between the torques acting on each sphere $\vec{\Gamma}_i$ and the velocities of each sphere can be derived in the form:

$$\vec{\Gamma}_i = \vec{D}_i \wedge \sum_{j=1}^{3} H_{ij}\vec{V}_j. \quad (2)$$

Since no external force is present, the system is torque- and force-free:

$$\sum_{i=1}^{3} \vec{F}_i = \vec{0} \text{ and } \sum_{i=1}^{3} \vec{\Gamma}_i = \vec{0}. \quad (3)$$

To solve the whole problem, the system was parameterized as follows: a reference frame relative to the device was defined, whose axes are parallel to those of the laboratory frame and whose origin is the centre P of the device. In that frame, the position of each sphere i is given by the angle θ_i defined in Figure 1. A local cylindrical coordinates system $\left(\vec{U}_{r_i}, \vec{U}_{\theta_i}\right)$ is defined for each sphere, so that the velocity of each sphere in the laboratory frame is given by

$$\vec{V}_i = \vec{V}_p + L\dot{\theta}_i\vec{U}_{\theta_i} \quad (4)$$

where $\vec{V}_p$ is the translation velocity of the centre P. During each step of the cycle, two other constraints are added; for example during the first step we set

$$\dot{\theta}_2 - \dot{\theta}_1 = -\omega. \quad (5)$$

and

$$\dot{\theta}_1 = \dot{\theta}_3. \quad (6)$$

The resulting system of equations was symbolically and numerically solved with *Mathematica*.

Figure 2 shows the total angle of rotation of the device during a complete four-step cycle as a function of the internal relative angular motion in an individual step for various values of the ratio $\frac{R}{L}$ when the whole system cannot undergo translational motion. The results show a significant dependence on the ratio $\frac{R}{L}$ and a close-to-quadratic variation of the angle of rotation with respect to the relative internal angular change for motions of small amplitude of internal change.

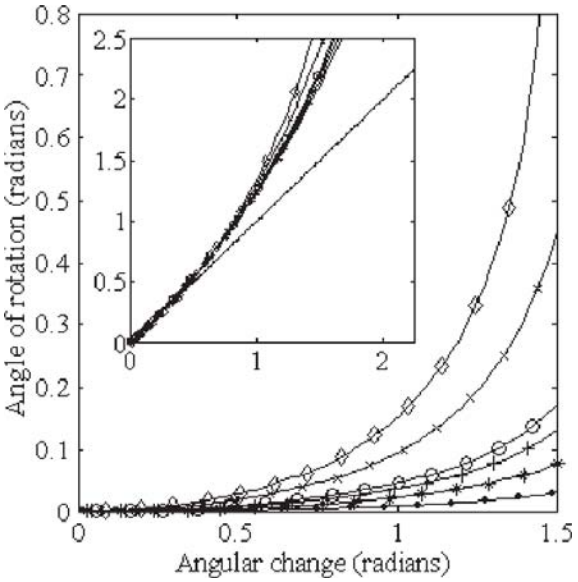

Fig. 2. Variation of the total angle of rotation during a cycle as a function of the internal angular change, when the device is not allowed to undergo translational motion. The different curves correspond to different values of ratio R/L: •0.02, ∗0.05, +0.08, ∘0.1, ×0.2, ◇0.3. The inset shows the scaled angle of rotation as a function of the square of the angular change (the scaling is indicated in the text). The solid line corresponds to a line of slope 1.

To gain further insight, we considered that the internal angle change is small enough for Taylor expansions to be valid. For small amplitudes of internal angular changes, an analysis of the equations of motion leads us to an expression for the rotation angle 2ε of the device after one cycle:

$$2\varepsilon = \frac{17}{16}\frac{\frac{R}{L}}{\left(3 - \frac{3\sqrt{3}}{8}\frac{R}{L}\right)}\theta^2 \approx \frac{17}{48}\frac{R}{L}\theta^2, \quad (7)$$

if $\frac{R}{L} \ll 1$, θ being the internal angular change.

The inset in Figure 2 represents 2ε scaled by the slope $\frac{17}{16}\frac{\frac{R}{L}}{\left(3-\frac{3\sqrt{3}}{8}\frac{R}{L}\right)}$ as a function of θ^2 for different values of $\frac{R}{L}$. As expected, the different curves are well superposed for small values of θ^2 and for all values of $\frac{R}{L}$.

If the center P is not kept fixed (Fig. 3), so that we now enforce zero net force as well as zero net torque, then it turns out that there is almost no dependence of the net rotation angle of the device on the ratio $\frac{R}{L}$. Since, according to the expression of the Oseen's tensor, the ratio $\frac{R}{L}$ characterizes the hydrodynamic coupling between the spheres, this coupling has almost no impact on the rotation of the device. In this case, quite analogous to the

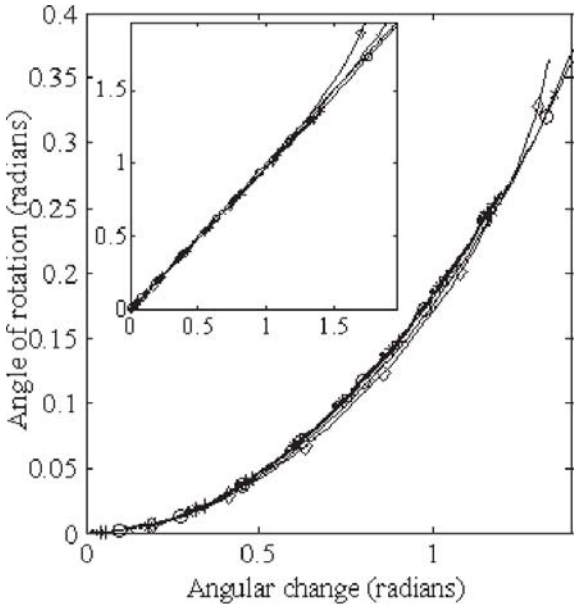

Fig. 3. Variation of the total angle of rotation during a cycle as a function of the internal angular change, when translational motion is allowed. The different curves correspond to different values of ratio R/L: $\bullet 0.02$, $*0.05$, $+0.08$, $\circ 0.1$, $\times 0.2$, $\diamondsuit 0.3$. The inset shows the scaled angle of rotation as a function of the square of the angular change (the scaling is indicated in the text). The solid line corresponds to a line of slope 1.

"falling cat problem" [15], the rotation is not due to interactions between the different spheres, but rather is due to the coupling between rotational and translational motions. Since there is no force and no torque the device can rotate, even if hydrodynamic coupling between the spheres is not considered. We also perform a Taylor expansion for small amplitudes of internal angular changes, which leads us to expression (8) for the rotation angle ε after one cycle:

$$2\varepsilon = \left(\frac{\sqrt{3}}{9} - \frac{3R}{48L}\right)\theta^2 \approx \frac{\sqrt{3}}{9}\theta^2, \qquad (8)$$

if $\frac{R}{L} \ll 1$, θ being the internal angular change.

The inset in Figure 3 represents 2ε scaled by the slope $\left(\frac{\sqrt{3}}{9} - \frac{3R}{48L}\right)$ as a function of θ^2 for different values of $\frac{R}{L}$. The different curves are well superposed for small and large values of θ^2 and for all values of $\frac{R}{L}$.

We have shown that using movements that are not kinematically reversible there is an almost perfect quadratic variation of the angle of rotation with respect to the relative internal angular change. In the literature on low-Reynolds-number propulsion, and for very different kinds of swimmers, under the Oseen or slender body description, the net translation speed is a quadratic function of the internal shape change or displacement [1,12–17]. Perhaps, not surprisingly, this quadratic dependency, which is the simplest one allowed in order to get beyond the constraint of kinematic reversibility, suggests that there may be an underlying universal feature derivable from the Stokes equations.

As a final remark, we note that certain molecular machines undergo ATP- or photochemically-driven rotational movements use a multi-step cycle in which individual subelements of the molecule undergo successive and kinematically non reversible changes of conformations [18,19] quite similar to the changes of conformation of the Purcell "rotator". Even if we have to keep in mind that at the nanoscale, Brownian motion is dominant, and that the continuous model of hydrodynamics we use here may begin to be flawed, it is tempting to think that such multistep cyclic molecular motors may involve mechanical principles not so unlike those described in this paper for rotation, via internal torques, in viscously dominated flows, so that overall rotation of these molecules occurs.

H.A.S. thanks ESPCI and J. Bibette and his research group for hospitality during the time when this research was initiated.

References

1. G.I. Taylor, P. Roy. Soc. Lond. A Mat. **209**, 447 (1951)
2. G.I. Taylor, in *Low Reynolds Number Flows* (The U.S. National Committee for Fluid Mechanics, 1966)
3. J. Lighthill, in *Mathematical Biofluiddynamics* (SIAM, 1975), Vol. 17
4. S. Childress, in *Mechanics of Swimming and Flying* (C.U. Press, 1981)
5. T.Y. Wu, Nav. Res. Rev. **26**, 12 (1973)
6. M. Ramia, D.L. Tullock, N. Phanthien, Biophys. J. **65**, 755 (1993)
7. C.H. Wiggins, D. Riveline, A. Ott, R.E. Goldstein, Biophys. J. **74**, 1043 (1998)
8. S.A. Koehler, T.R. Powers, Phys. Rev. Lett. **85**, 4827 (2000)
9. S. Camalet, F. Julicher, J. Prost, Phys. Rev. Lett. **82**, 1590 (1999)
10. J.E. Avron, O. Gat, O. Kenneth, Phys. Rev. Lett. **93,** 186001 (2004)
11. E.M. Purcell, Am. J. Phys. **45**, 3 (1977)
12. L.E. Becker, S.A. Koehler, H.A. Stone, J. Fluid. Mech. **490**, 15 (2003)
13. A. Najafi, R. Golestanian, Phys. Rev. E **69**, 062901 (2004)
14. J.E. Avron, O. Kenneth, D.H. Oaknin, `arXiv: math-ph/0501049` (2005)
15. J.E. Avron, O. Gat, O. Kenneth, U. Sivan, Phys. Rev. Lett. **92**, 040201 (2004)
16. H.A. Stone, A.D.T. Samuel, Phys. Rev. Lett. **77**, 4102 (1996)
17. G.J. Hancock, P. Roy. Soc. Lond. A Mat. **217**, 96 (1953)
18. N. Koumura, R.W.J. Zijlstra, R.A. van Delden, N. Harada, B.L. Feringa, Nature **401**, 152 (1999)
19. K. Kinosita, R. Yasuda, H. Noji, K. Adachi, Philos. T. Roy. Soc. B **355**, 473 (2000)